2020 IEEE/RSJ International Conference on Intelligent Robots and Systems (IROS)
October 25-29, 2020, Las Vegas, NV, USA (Virtual)

The AmphiSTAR High Speed Amphibious Sprawl Tuned Robot: Design and Experiments

Avi Cohen, and David Zarrouk

***Abstract*—This paper details the development, modeling and performance of AmphiSTAR, a novel high-speed amphibious robot. The palm size AmphiSTAR, which belongs to the family of STAR robots, is a "wheeled" robot fitted with propellers at its bottom that allow it to crawl on the ground and run (i.e. hover) on water at high speeds. The AmphiSTAR is inspired by two members of the animal kingdom. It possesses a sprawling mechanism inspired by cockroaches, and it is designed to run on water at high speeds like the Basilisk lizard. We start by presenting the mechanical design of the robot and its control system. Then we model AmphiSTAR when crawling, swimming and running on water. We then report experiments on the robot to measure its lift and thrust forces in its on-water running mode and evaluate its energy consumption. The results show that in the on-water running mode, the lift forces are a function of the work volume of the propellers whereas the thrust forces are a linear function of the propellers' rotating speed. Based on these results, the final version of the 3D printed robot was built and experimentally tested in multiple scenarios. The experimental robot can crawl over the ground with performances similar to the original STAR robot and can attain speeds of 3.6 m/s. The robot can run continuously on water surfaces at speeds of 1.5 m/s. It can also swim (i.e. float while advancing by rotating its propellers) at low speeds and transition from swimming to crawling (see video).**

***Index Terms*— Crawling Robot, Swimming Robot, Amphibious Robot, Basilisk Lizard.**

I. INTRODUCTION

Miniature crawling robots that can move within unstructured environments for search and rescue, agriculture, excavation, surveillance, security and reconnaissance missions have been developed for the last two decades. Their small size, low weight and high navigability enable their deployment in large numbers to quickly inspect large areas. Much effort has been invested in reducing their size, increasing their speed and lowering their energy consumption. Examples of crawling robots include Mini-Whegs [1], Dyna-RoACH [2], DASH [3], iSprawl [4], OctoRoACH [5], RHex [6], STAR [7], 1STAR [8] TAYLRoACH [9] and RSTAR [10]. Many substantial advances have been made in the design of these robots using passive mechanics, minimal actuation [11] and reconfigurable mechanics [12]-[17].

Most of these crawling robots are primarily designed for crawling over dry land but cannot propel themselves in aquatic environments or in the presence of water or mud (during floods for example) which can cause sliding or wet their electronics. Floyd and Sitty [18] developed an experimental legged robot to analyze the dynamics of the Basilisk lizard [19]. Their results suggest that a legged robot running on water must weigh a few grams only, implying that it will not be able to carry batteries and cameras. Robots must be even lighter if they rely on water surface tension for floating and moving [20][21].

Figure 1. The AmphiSTAR is a newly developed STAR robot fitted with a sprawling mechanism and four propellers at its bottom. The two propellers at each side are actuated using a single brushless motor. The robot can crawl over the ground or swim and run over water.

Larger robots achieved better performance both in swimming and crawling. Undulating robots such as snake-like [22] and salamander-like [23] robots achieved respectively top speeds of up to 0.3 m/s and 0.5 m/s in water. The salamander was also able to crawl at 0.5 m/s on land. The minimally actuated Velox [24] reached a swimming speed of 0.5 m/s but only a few cm/s on land, whereas the SAW robot [25] reached speeds of 50 cm/s on land and only 6 cm/s in water. In a different approach, the legged AQUA robot [26] uses its legs to crawl on land and as fins for swimming on the water's surface and underwater. The AQUA robot has a reported underwater speed of 1 m/s. Although, it shares a similar design to RHex, its fin like legs (not C shape like) would substantially reduce its speed and stability on land (its land speed is not reported in literature).

While nature offers many solutions for crawling and swimming, bio-inspired robots are still trailing behind. *Nothing is like the real thing* noted Triantafyllou et al. in 1995 [27]. Since then, bio-inspired robots keep closing the gap but are still unable to match the performance of their biological counterparts. Legged robots, for example, did not replace wheeled and tracked vehicles in real search and rescue applications. The same is also correct for swimming. In a very recent study, Struebig et al. [28] showed that although, theoretically speaking, undulating mechanism are supposedly more efficient than propellers (a whale can reach

A. Cohen and D. Zarrouk are both associated with the Department of Mechanical Engineering at Ben Gurion University of the Negev, Israel. (zadavid@bgu.ac.il).

an efficiency of up to 85% [29]) , actual undulating systems are still unable to match the efficiency of fish and even fall behind the efficiency of propellers (nearly 50%).

In previous works [7], [8], [11] and [30], we developed multiple variations of the STAR robots. The original STAR was actuated by 3 motors and introduced a sprawling mechanism to change its dynamics between the lateral and sagittal planes. The minimally actuated 1STAR, with a fixed sprawl, is actuated by a single motor. The reconfigurable RSTAR has a four bar mechanism, and the flying FSTAR can drive and fly.

The new amphibious STAR robot (AmphiSTAR) presented in this paper (Figure 1) belongs to the same family of STAR robots; i.e., it can also vary its sprawl angle. However, the AmphiSTAR has 4 propellers instead of whegs/wheels which enable it to crawl on the ground and swim (i.e. float and advance by slowly rotating its propellers) at low speed or run (i.e. hover) on the water's surface at high speeds. The total length of the robot is 22.5 cm (26.5 cm including its floating tanks) and its width in the flat mode is 26.5 cm. The total weight of the robot including its batteries and control board is 246 grams.

This paper is organized as follows. We present the mechanical design of the AmphiSTAR and its components in Section II. The dynamic model of the robot crawling over ground and water is presented in Section III and the results of the force and torque experiments in Section IV. Finally, experiments presenting the robot crawling over the ground and swimming and running on water are presented in Section IV.

II. DESIGN AND MANUFACTURING

The primary design goals of the AmphiSTAR are to achieve high performance in swimming, running on water and crawling over land. Its weight was lowered to ensure it can lift itself above water level when rotating its propellers at high speeds. The length of the robot is 22.5 cm and its total weight is 246 grams. The weight of all the mechanical components of the robot is 149 grams. Its battery weighs 43 grams and its electronic components (receiver, controller, ESC, servo and brushless motors) weigh 54 grams.

A. Robot Design

The AmphiSTAR is composed of a main rigid body which houses the controller and receiver, and the servo motor which actuates the sprawl of the robot. The robot has two arms which hold the motor housing and propellers. The two propellers at each side are actuated by a single brushless motor. The sprawl mechanism tilts the two arms which move symmetrically relative to its center body. At zero sprawl, the axis of the propellers is vertical. When tilted, the propellers provide the required thrust forces to advance. The propellers also provide the lift forces when they are rotating at high speeds.

1) The Sprawling Mechanism

Similar to the previous STAR robots, we define the sprawl angle ρ as the relative angle between the arms which hold the motors and propellers to the main body. A zero sprawl occurs when the arms are parallel to the body and a positive sprawl occurs when the arms are rotated downwards.

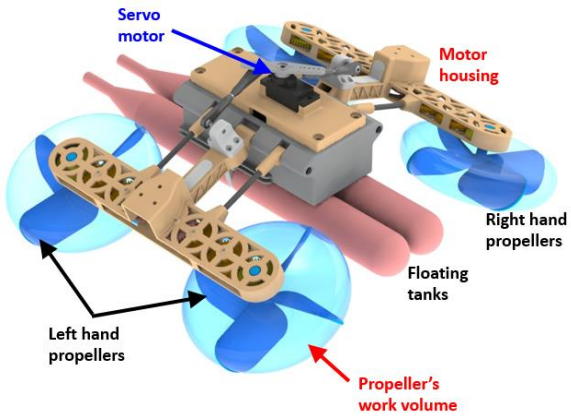

Figure 2. The mechanical design of the AmphiSTAR robot and its main components.

The sprawl mechanism is kinematically a three-dimensional four bar mechanism (two identical mechanisms on each side to ensure symmetry). The sprawl is actuated using a servo motor which rotates a small arm. A push rod is attached to the servo motor's arm tip with spherical joints. As the servo rotates its arm, it pulls or pushes the arms of the robot to fix their sprawl at the desired angle. More on the design of the sprawl mechanism and the forces needed to actuate it can be found in our previous work [30]. The sprawl angle in this design can be varied in the range of 0 to 25 degrees as shown in Figure 3.

2) The Arms, Motor Housing and Gear Boxes.

The propellers at each side are powered by a single motor. A gear ratio of 1:16.7 is used to reduce the speed of the propellers and increase the torque. The torque is transmitted from the motor to the propellers via 4 consecutive spur gears.

3) Propellers

The custom- made propellers (two on each side) have four blades each. The propellers on the right side and left side of the robot have opposite pitches, so that when they rotate in opposite directions they both produce lift forces. The 3D printed custom designed propellers were optimized along preliminary experiments to improve their reliability in order to withstand the ground impacts and water pressure. Their diameter is 9 cm and their height is 2 cm while their blade thickness is 1.5 mm. Their angle of attack is variable, ranging from 40 degrees at the center to 65 degrees on the external diameter. The shallower angle of attack at the center allows for increased strength against breaking and bending. While increasing the diameter of the propellers would increase their lift forces, they must still be distanced to reduce their interference (which produce opposing/resisting flows). The distance between the centers of the propellers was fixed at two diameters and the distance between their tips is nearly a single diameter.

A. Actuation and Control

The AmphiSTAR is actuated with two brushless motors that are used to rotate the propellers (one at each arm) and a servo motor which actuates the sprawl mechanism. The brushless motors (2900RPM/V) can operate at a nominal

voltage of 11.1 Volts. Each motor generates a torque of 0.4 Ncm and can reach a maximum speed of 35000 RPM (see the torque and speed experiments in Section IV).

The robot is fitted with a flight controller and receiver. The flight controller (HGLRC F4.V2) ensures that the robot can be controlled by a human operator using a joystick. The servo motor (HD-1810MG) has a rotational range of 145 degrees, weighs 16 grams and produces a torque of 0.31 Nm.

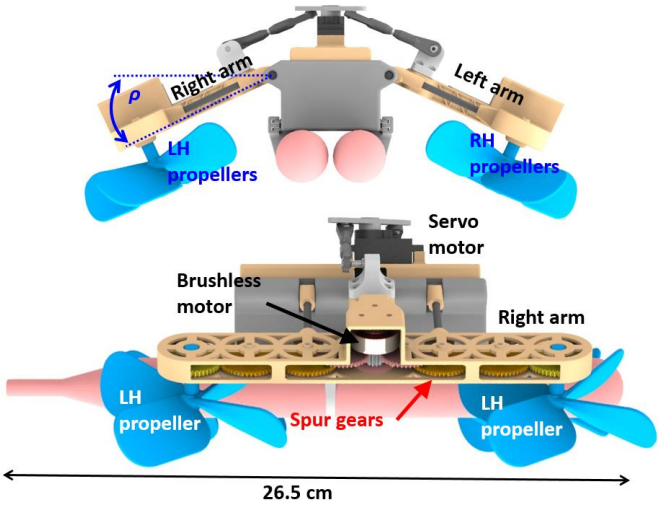

Figure 3. The sprawl mechanism, actuated using a servo motor, has a range of 25 degrees. The torque of the motors is transferred to each propeller using 4 consecutive gears with a gear reduction ratio of 1:16.7. Right hand propellers are attached to the left arm and left hand propellers to the left arm.

B. Manufacturing

Most of the mechanical parts of the AmphiSTAR are manufactured using in-house 3D printing. We used a Form 2 printer (SLA) whose accuracy is roughly 0.1 mm for the arms and small components and an Ultimaker 5 printer (Fuse Deposition Modeling - PLA), whose accuracy is roughly 0.2mm, for the main body. We invested considerable effort in simplifying the design of the robot and reducing its weight to increase its speed while reducing its power consumption and to ensure it can run on water.

III. Robot Model

In this section, we analyze the kinematics and dynamics of the robot crawling over the ground and when swimming or running on the water's surface. Throughout the analysis, we assumed that the sprawl angle ρ was 25 degrees which is the maximum angle to generate enough lift force to sustain the robot above the water level while running over water (nearly 2.5 Newtons).

A. Running on Ground

The robot uses a differential drive, where each set of propellers on each side is actuated by a separate motor. The ground crawling speed of the robot is a function of the angular speed of the motor and its sprawl angle. A gear ratio of 1:16.7 is used to increase torque and reduce speed. The ground speed V_{Ground} of the robot is limited by the speed of the propellers' tips:

$$V_{Ground} \le \dot{\alpha} \cdot R(\rho) \qquad (1)$$

where $\dot{\alpha}$ is the angular speed of the propellers and $R(\rho)$ is their effective radius; i.e., the distance from the axes or rotation to the contact point with the ground. The effective radius $R(\rho)$ ranges from 32.3 cm to 35.9 cm for the sprawl which ranges from 13 degrees (the minimum sprawl for which the propeller can contact the ground) to 25 degrees.

1) Thrust Forces in Swimming Mode

The thrust is generated on the external side (right) of the propeller whereas the internal side (left) resists the motion (see Figure 5). If the propeller is tilted by ρ, the total force difference acting on the propeller (right side minus left side) is equal to the weight of the displaced water volume ΔV. Assuming that the propeller is nearly cylindrical, the vertical force difference ΔF is:

$$\Delta F = \rho_w g \Delta V \approx 2\rho g A \cdot R \sin(\rho) \qquad (2).$$

Where A and R are respectively the disk area and radius of the propeller. Our assumption, which is supported by the results in section IV.C, is that the thrust force is proportional to ΔF and therefore proportional to $\sin(\rho)$.

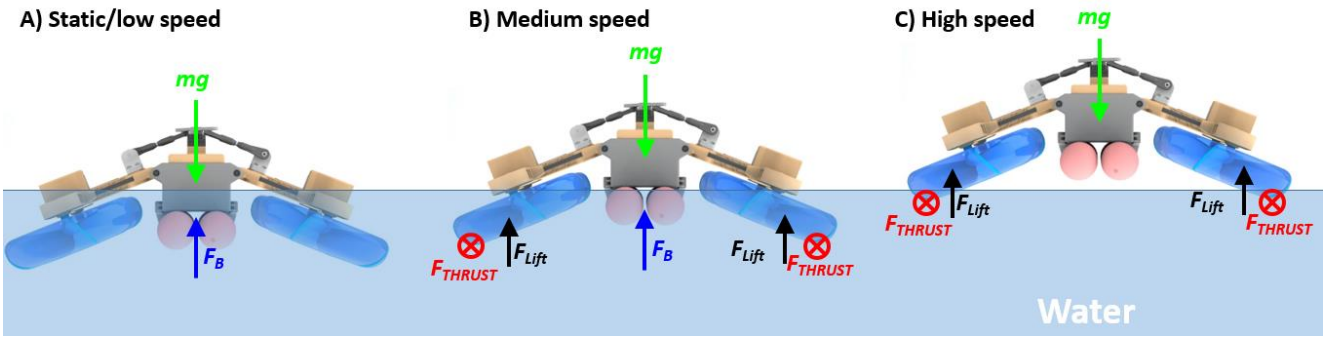

Figure 4. The robot in swimming mode. At low speed (A), the robot is static or swimming at low speed. In (B), the robot is at medium speed and in (C), the robot is in running on water mode.

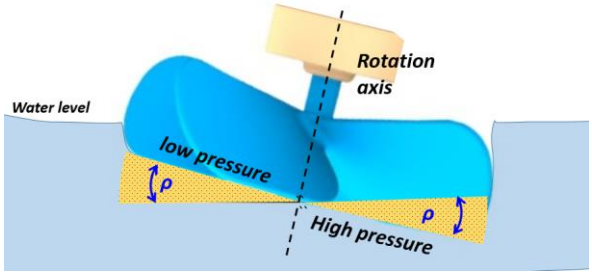

Figure 5. pressure difference of the two sides of the propeller in sprawled mode.

2) Running on Water

At high rotation speeds (exceeding 600 RPM), the propellers displace nearly all the water from their work volume. As such, the water will exert lift forces on the robot whose value is equal to the weight of the displaced water. Figure 6 presents a comparison between the forces acting on the robot when the robot is not actuated and when it is actuated, as a function of its depth (ρ=25 degrees). The volumes of water were obtained from the SolidWorks measurement properties function. The comparison shows that if the robot is not actuated, the lowest tip of its propellers will be immersed in 45 mm in water whereas the lowest depth will be 23 mm when actuated. Therefore, actuating the propellers at full speed will result in lifting the body of the robot by 22 mm relative to water level (this result was observed experimentally in Section IV).

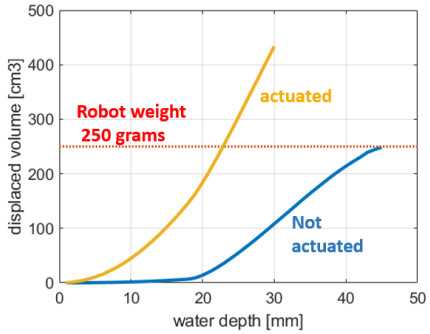

Figure 6. A comparison of the displaced volume of water when the robot is actuated versus not actuated.

IV. Force, Torque and Power Experiments

This section presents the experiments conducted to measure the lift forces as well as the torques generated by the motors as a function of the rotation speed, the size of the propellers and the thrust forces in the sprawl mode.

A. Experimental Setup

The experimental system was composed of a single motor house fitted with two propellers (identical to one side of the robot) immersed in a water tank. The motor house is held by a rigid arm attached to a 6 DOF Nano 25 force sensor whose accuracy is 0.01 N. A rotational joint makes it possible to rotate the motor house and mimic the behavior of the propellers' sprawled configuration. Throughout the experiments, the rotational speed of the propellers was controlled using a Teensy 3.5 controller, and the rotation speeds (using the encoder), forces and torques were continuously measured and saved for post processing. In the experiments, 3 propellers with different radii were used. The largest propeller was identical to the one eventually used in the actual robot.

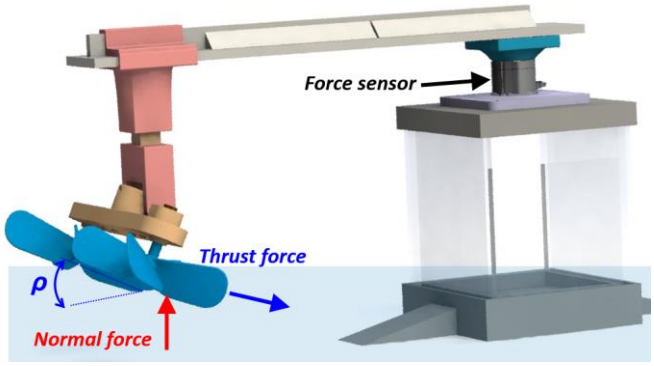

Figure 7. The experimental system used to measure the lift and thrust forces and the torque of the robot as a function of the radius and rotational speed of the propellers.

B. Lift and Torque as a Function of the Rotational Speed

The lift forces and torques were measured as a function of the angular speed (in RPM) at zero sprawl angle. The propellers were fully plunged into the water until their tips were just below the surface (see video).

Figure 8 presents the torque output of the propellers and the lift forces in the range of 100 to 1000 RPM as measured by the Nano 25 force sensor. The lift force and torque initially increased almost linearly until they reached the range of 400 RPM. Beyond that speed, the lift forces increased at a lower rate up to 600 RPM. Above 600 RPM, the force and torque remained nearly constant. As discussed in Section III, this is due to the fact that since the propeller is rigidly fixed in the vertical direction, it displaces all the water from its working space at nearly 600 RPM. Hence, beyond this rotation speed, the water has been fully removed from the work volume and the lift force cannot increase. The maximum average measured force is 1.5 N. The torque exhibits a similar behavior and does not increase beyond the rotational speed of 600 RPM. The maximum average measured torque is 0.06 Nm. The mechanical output power consumption at 600 RPM is 7.6 Watts (3.8 Watts for each side).

A. Influence of the Size of the Propellers and their Depth in Water on the Lift Force

In the previous experiment, we found that the lift forces remain constant beyond 600 RPM. In order to experimentally validate the hypothesis that the lift forces are equal to the weight of displaced water, we printed propellers with three different radiuses *R* (35 mm, 39 mm, and 45 mm). The different propellers were plunged in the water at 4 different depths: starting from 9 mm (nearly half way through water) to 14 mm, to 19 mm and finally 24 mm. In the largest depth, the water level was nearly in contact with the motor housing. Along the experiment, the propellers were commanded to rotate at 1000 RPM with close loop control using the Teensy 3.5 controller while the forces and

torques are measured and saved at 100 Hz. Figure 9 presents the measure lift forces of the medium size propeller as a function of the time, for four different depths.

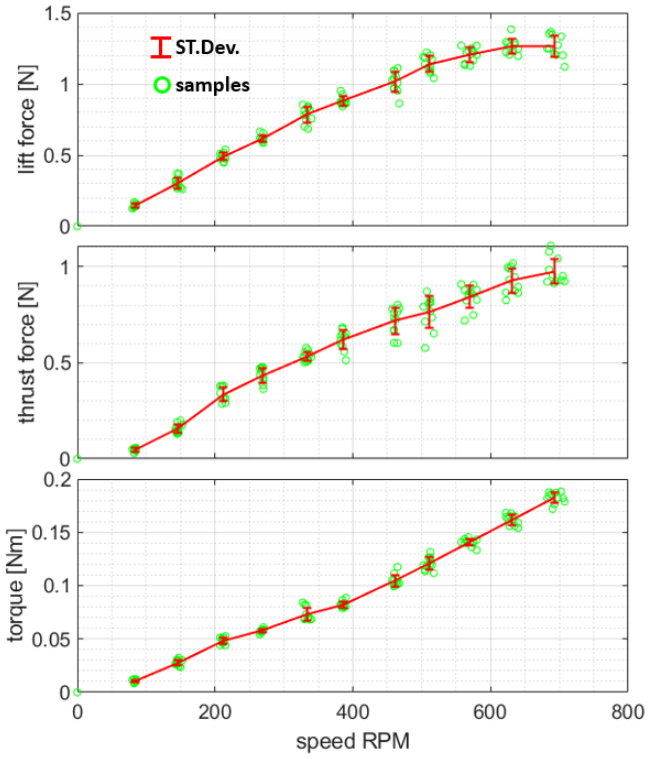

Figure 8. Lift and thrust forces as a function of the speed (the sprawl was set at 25 degrees).

To compare the experimental results to theoretical expectations, the work volume of the 3 propellers at the 4 different depths was measured using the Solidworks CAD (similar to Figure 6). The actual volume of the propeller that was below the water level was subtracted from the work volume. This was done because after the water is displaced it ceases to apply buoyancy forces on the propellers.

The observed forces and a comparison to theoretical expectations are presented in Figure 10 and Table I for all 12 experiments (4 depths for each of the three propellers).

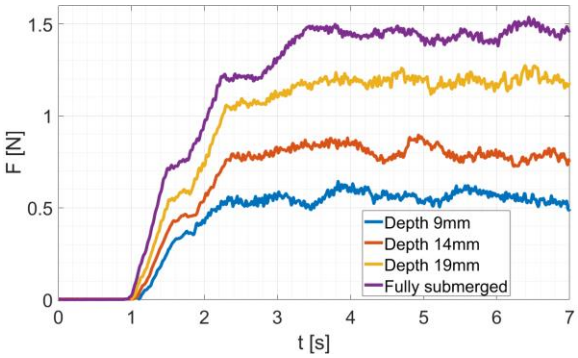

Figure 9. Lift forces as a function of the depth of the propeller at 1000 RPM on the medium propeller.

The measured forces were smaller than the theoretical estimate and the average percentage error was 16% whereas the correlation between the average measured force and the theoretical force is R=0.984. The difference between the estimated and measured force may have been due to the fact that during propeller rotation, some water kept leaking into their work-volume and reduced the lift force.

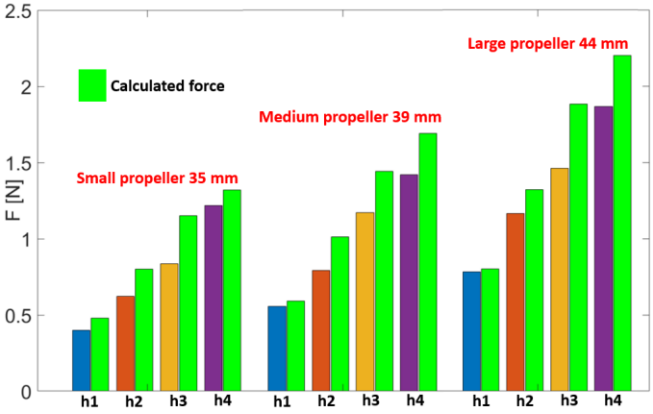

Figure 10. The observed and theoretical lift forces as a function of the water depth and propeller sizes.

B. Lift and Thrust Forces in the Sprawled Configuration

Since the robot can only advance in the sprawl configuration, we measured the thrust forces of the robot as a function of the rotational speed of the propellers when the sprawl angle was at 0, 10, 20 and 30 degrees.

The results, presented in Figure 12, show that the lift force continued to increase until the range of 600 RPM (similarly to zero sprawl) and retain its value for higher speeds. Note

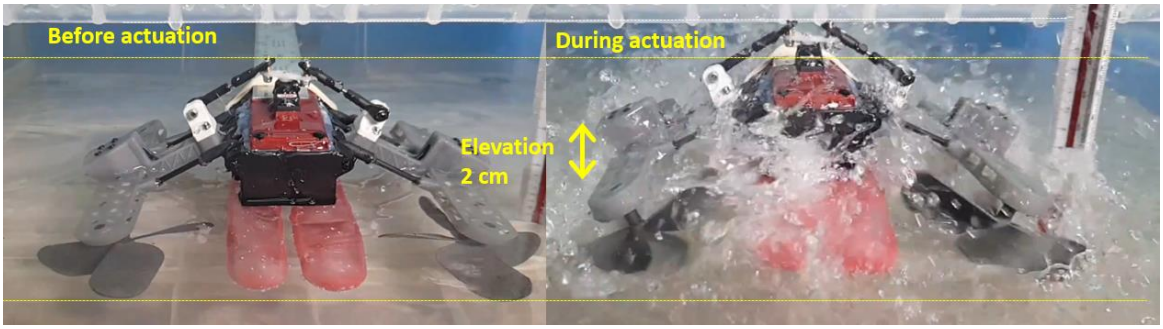

Figure 11. The robot elevation is measured when the robot is passively floating over the water (Left) and when it is actuated at full motor speed (Right).

that, as predicted by our model, the thrust forces for 20 degrees sprawl is twice large than the 10 degrees case. The increase between 20 to 30 degrees is 18% only (instead of sin(30°)/sin(20°)=46%). Probably due to the fact that the propeller is becoming like a wheel. A low sprawl can be used for travelling with payloads at low speeds whereas the higher sprawl can be used to travel a higher speeds.

C. Robot Elevation When on Water

In this experiment (Figure 13), the robot was fixed to a beam attached to a rotational joint. The length of the beam was nearly 50 cm, so that when the robot was actuated, it could not advance but only lift its body relative to the water and tilt slightly upwards (pitch). At the beginning of the experiment, the robot was floating over the water using buoyancy forces alone. The robot was then actuated at max power and filmed at 240 FPS. In the experiment, the actuation of the robot elevated the robot by 1.8 cm and the floating tanks were above water level as a result of the lift forces of the propellers (see video).

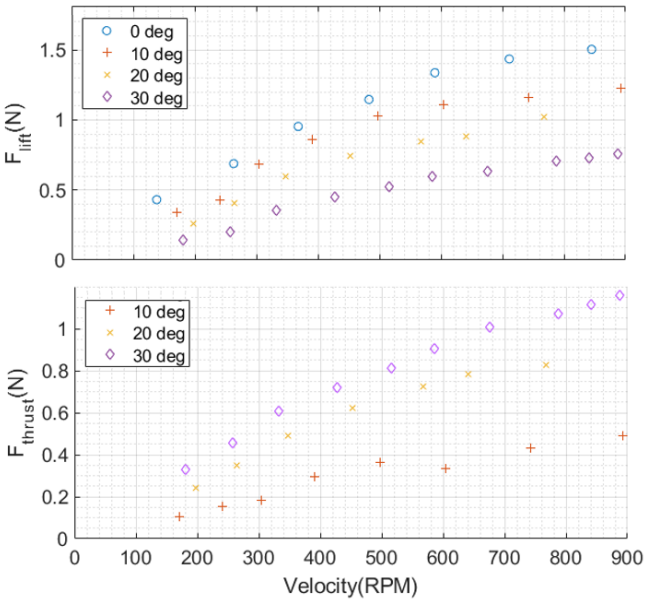

Figure 12. The lift and thrust for 0, 10, 20 and 30 degrees sprawl angles as a function of the rotation speed.

V. Robot Performance

In this section we tested the AmphiSTAR while crawling over different surfaces in the swimming and running on water modes. In all the experiments presented in this section, the robot was controlled by a human operator (combined with the onboard flight controller). The robot exhibited high reliability throughout the experiments, in that it successfully and repetitively performed the experiments while requiring no maintenance during filming (excluding replacing batteries).

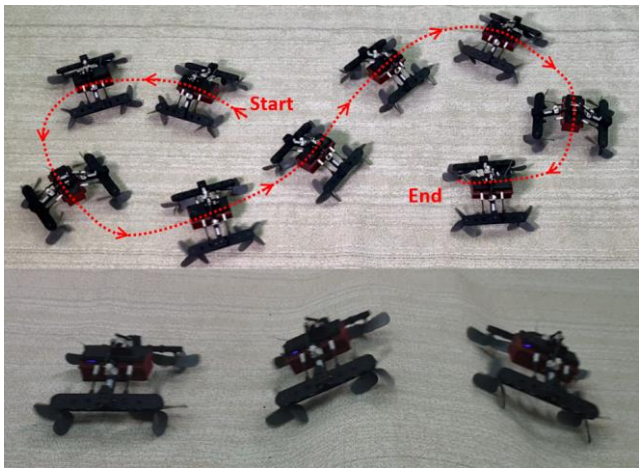

Figure 13. Top) The AmphiSTAR rotating clockwise and then counter clockwise. Bottom. The AmphiSTAR climbing over an incline (see video).

A. Crawling Experiments

1) In-Lab Crawling Experiments

We first tested the robot in the laboratory over carpet surfaces. The robot was turned clockwise and counter clockwise at a turn radius of nearly 0.2 m. The robot was then successfully driven over an incline.

2) Outdoor Crawling Experiments

The AmphiSTAR was tested outdoor crawling over different surfaces. In the Figure 14, the AmphiSTAR is shown crawling over different surfaces and transitioning from concrete to ground, grass and gravel.

Figure 14. Top) The AmphiSTAR successfully crawling over different challenging surfaces including gravel, dirt, grass and mud (see video).

Due to space constraints in the laboratory, the speed of the robot could not be measured using traditional tracking systems. For this reason, we filmed the robot running at high speed over grass and estimated its speed by analyzing video frames. After initially accelerating for five meters, the robot reached a speed of more than 3.6 m/s (Figure 15).

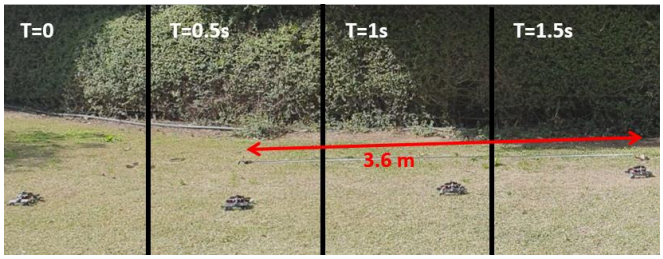

Figure 15. The AmphiSTAR crawling over grass at 3.6 m/s (see video).

B. Swimming and Running On Water Experiments.

1) In-Lab Swimming Experiments

In the first experiment, the robot was placed on an incline and driven towards a small pool of water. The robot was actuated at low speeds so its propellers could act as fins and its air tanks provided the floating forces (see video). The robot crawled slowly over the ramp towards the water, swam forward as its propellers acted as fins, then rotated and returned back to the ramp to climb back onto the ramp, (see video). In the second experiment also presented in video, the AmphiSTAR was driven until it fell into the water. At this point, the propellers were actuated at high speed. The lift forces elevated its body above the water and the robot ran on the water and then climbed over the ramp at high speed.

1) Outdoor Water Running Experiments

After successfully testing the robot in the small pool, the robot was taken outdoors to a large puddle with muddy edges measuring up to 20 cm in depth and into a small artificial pond (see Figure 16 and video). The robot successfully crawled over the mud and ran on water at estimated speeds of up to 1.5 m/s. In the artificial pond, the robot crossed (18 m) multiple times while running on water in windy conditions against the current.

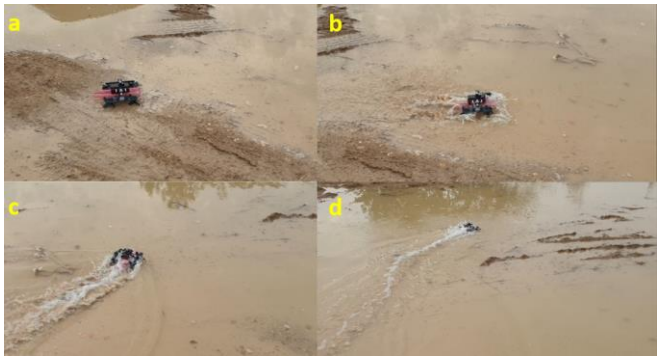

Figure 16. AmphiSTAR transitioning from crawling to swimming and then crawling (see video).

VI. CONCLUSION

In this paper we presented a novel highly mobile amphibious STAR robot (AmphiSTAR) that can crawl on the ground, swim and run on water at high speeds. The AmphiSTAR can be used for excavation, as well as agricultural and search and rescue applications where both crawling and swimming are required. The 3D printed AmphiSTAR is a "wheeled" robot but draws its inspiration from cockroaches (for sprawling) and from the Basilisk lizard (for running on water). It has a simple design and easy to control. It weighs 246 grams, and is fitted at its bottom with 4 propellers whose axes can be tilted using the sprawl mechanism. The propellers act as wheels over ground, as fins to propel the robot over water while swimming and running on water when the propellers are actuated at high speeds.

The robot is fitted at its bottom with air tanks which provide buoyancy to keep the robot floating at low speeds and as a precaution against sinking in the case of lost communication or if the motor or controllers malfunction.

Using its tilted propellers, the robot can crawl over tiles, ground, mud, and grass at speeds of up to 3.6 m/s. It can run on water at speeds of up to 1.5 m/s and even against the currents. Since the robot can float on the water using its air tanks, it can transition smoothly between high speeds when running on water, to lower speeds swimming and from crawling to swimming and vice versa.

When running at high speeds on water, the lift forces of the robot were equal to the weight of the volume of water displaced by the propellers with a correlation coefficient of R=0.984. Increasing the rotation speed of propellers in excess of 600 RPM would not increase the lift forces but would increase the torque and thrust forces of the robot. Therefore, to increase the weight it can carry, its propellers must be enlarged. The energy consumption of the robot when running at top speed in water is 7.6 Watts, which translates into a mechanical COT of 2.13. As the majority of the generated force is used to keep the robot afloat, it is expected that the maximum thrust efficiency of this design will be smaller than half of the efficiency of a regular propeller (which is usually 50%). Another disadvantage of the robot is that it is not eco-friendly in the sense that it produces much noise and water perturbation and is not suitable for exploration wild life for example.

Our future research will focus on the scalability of the robot and on underwater swimming.

ACKNOWLEDGMENTS

This study was supported in part by the Pearlstone center for aeronautical studies and by the Helmsley Charitable Trust through the Agricultural, Biological and Cognitive Robotics Initiative, and by the Marcus Endowment Fund, both at Ben-Gurion University of the Negev.

REFERENCES

[1] J. M. Morrey, B. Lambrecht, A. D. Horchler, R. E. Ritzmann, and R. D. Quinn, "Highly mobile and robust small quadruped robots", IEEE Int. Conf. on Intelligent Robots and Systems, Vol. 1, pp. 82-87, 2003.

[2] A. M. Hoover, S. Burden, X. Y. Fu, S. S. Sastry, and R. S. Fearing, "Bio-inspired design and dynamic maneuverability of a minimally actuated six-legged robot", IEEE Int. Conf. on Biomedical Robotics and Biomechatronics, pp. 869-873, 2010.

[3] P. Birkmeyer, K. Peterson, and R. S. Fearing, "DASH: A dynamic 16g hexapedal robot", IEEE Int. Conf. on Intelligent Robots and Systems, pp. 2683-2689, 2009.

[4] S. Kim, J. E. Clark, and M. R. Cutkosky, "iSprawl: Design and turning of high-speed autonomous open-loop running", *The Int. Journal of Robotic Research*, Vol. 25, No.9. pp. 903-912, 2006.

[5] A. O. Pullin, N. J. Kohut, D. Zarrouk, and R.S. Fearing, "Dynamic Turning of 13cm robot comparing tail and differential drive", IEEE Int. Conf. on Robotics and Automation, pp. 5083-5093, 2012.

[6] K. C. Galloway, G. C. Haynes, B. D. Ilhan, A. M. Johnson. R. Knopf, G. Lynch, B. Plotnick, M. White, and D. E. Koditschek, "X-RHex: a highly mobile hexapedal robot for sensorimotor tasks", University of

Pennsylvania Technical Report, 2010.
[7] D. Zarrouk, A. Pullin, N. J. Kohut, and R. S. Fearing, "STAR - Sprawl Tuned Autonomous Robot", IEEE Int. Conf. on Robotics and Automation, pp. 20-25, 2013.
[8] D. Zarrouk, and R. S. Fearing, "Controlled In-Plane Locomotion of a Hexapod Using a Single Actuator", IEEE *Trans. on Robotics*, Vol. 31, No. 1, pp. 157-167, 2015.
[9] N. J. Kohut, A. Pullin, D. Haldane, D. Zarrouk, and R. S. Fearing, "Precise Terrestrial Turning Using an Inertial Appendage", IEEE Int. Conf. on Robotics and Automation, pp. 3399-3306, 2013.
[10] D. Zarrouk, and L. Yeheskel, "Rising STAR, a highly reconfigurable sprawl tuned autonomous robot", IEEE, *Robotics and Automation Letters*. Vol. 3, No.3, pp. 1888-1895, 2014. DOI. 10.1109/LRA.2018.2805165.
[11] P. K. Karidis, D. Zarrouk, I. Poulakakis, R. S. Fearing, and H.G. Tanner, "Planning with the STAR(s)", IEEE Int. Conf. on Intelligent Robots and Systems, pp. 3033-3038, 2014.
[12] J. T. Karras, C. L. Fuller, K. C. Carpenter, A. Buscicchio, D. McKeeby, C. J. Norman, C.E. Parcheta, I. Davydychev, and R. S. Fearing, Pop-up Mars Rover with Textile-Enhanced Rigid-Flex PCB Body, IEEE Int. Conf. Robotics and Automation, Singapore, May 2017.
[13] Y. S. Kim, G. P. Jung, H. Kim, K. J. Cho, and C. N. Chu, "Wheel Transformer: A Wheel-Leg Hybrid Robot With Passive Transformable Wheels", IEEE trans. On Robotics, Vol. 30, N6, pp. 1487-1498, 2014.
[14] M. J. Spenko, G. C. Haynes, J. A. Saunders, M. R. Cutkosky, A. A Rizzi, R. J. Full, and D. E. Koditschek, "Biologically Inspired Climbing with a Hexapedal Robot," *Journal of Field Robotics*, Vol. 25, No. 4, 2008.
[15] N. Tan, R. E. Mohan, and K. Elangovan, "Scorpio: A Biomimetic Reconfigurable Rolling-Crawling Robot", *International Journal of Advanced Robotic Systems*, DOI: 10.1177/1729881416658180, 2016.
[16] S. C. Chen, K. J. Huang, W. H. Chen, S. Y. Shen, C. H. Li, and P. C. Lin, "Quattroped: A Leg–Wheel Transformable Robot", *IEEE/ASME trans. On Mechatronics*, Vol. 19, No. 2, 2014.
[17] Y. Sun, and S. Ma, "Decoupled Kinematic Control of Terrestrial Locomotion for an ePaddle-Based Reconfigurable Amphibious Robot", IEEE International Conference on Robotics and Automation, pp. 1223-1228, 2011.
[18] S. Floyd, & M. Sitti, "Design and Development of the lifting and propulsion mechanism for a biologically inspired water runner robot", IEEE Transactions on Robotics, vol. 24. no. 3, pp. 698-709, 2008.
[19] J. Glasheen, and T. McMahon, "A hydrodynamic model of locomotion in the Basilisk lizard," Nature, vol. 380, pp. 340-342, 1996.
[20] Y.S. Song, M. Sitti, "Surface tension driven biologically inspired water strider robot", IEEE, Transactions on Robotics, vol. 23, no. 3, pp. 578-589, 2007.
[21] O. Ozcan, H. Wang, J. D. Taylor, and M. Sitti, "STRIDE II: a water strider-inspired miniature robot with circular footpads", International Journal of Advanced Robotics Systems, pp. 1-11, 2014, DOI: 10.5772/58701.
[22] A. Crespi, and A.J. Ijspeert, "Online optimization of swimming and crawling in an amphibious snake robot", CLAWAR, pp. 19-27, 2006.
[23] A. Crespi, K. Karakasiliotis, A. Guignard, A.J. Ijspeert, "Salamandra Robotica II: An Amphibious Robot to Study Salamander-Like Swimming and Walking Gaits", IEEE Transactions on Robotics, vol. 29, no.2, pp. 308-320, 2012. doi: 10.1109/TRO.2012.2234311
[24] Velox Robot: youtube: https://www.youtube.com/watch?v=evQF7SJt2p0
[25] D. Zarrouk, M. Mann, N. Degani, T Yehuda, N. Jarbi, A. Hess, "Single actuator wave-like robot (SAW): design, modeling, and experiments", *Bioinspiration and Biomimetics*, vol. 1, no. 1, pp. 1-14, 2016. doi:10.1088/1748-3190/11/4/046004
[26] G. Dudek et al. "AQUA: an amphibious autonomous robot", *IEEE Computer*, pp. 46-53, 2007.
[27] M. S. Triantafyllou and G. S. Triantafyllou, "An efficient swimming machine", Scientific American, vol. 272, pp. 64-70, 1995.
[28] K. Struebig, B. Bayat, P. Eckert, A. Looijestijn, T. C. Lueth, and A. J. Ijspeert, "Design and development of the efficient anguilliform swimming robot - MAR", Bioinspiration and Biomimetics, vol. 15, 035001.
[29] L. Schouveiler, F. S. Hover, and M. S. Triantafyllou, "Performance of flapping foil propulsion", Journal of Fluids and Structures, vol. 20, pp. 949-959, 2005.
[30] N. Meiri, and D. Zarrouk, "Flying STAR, a hybrid crawling and flying sprawl tuned robot, IEEE Int. Conf. on Robotics and Automation, pp. 5302-5308, 2019.

VII. APPENDIX

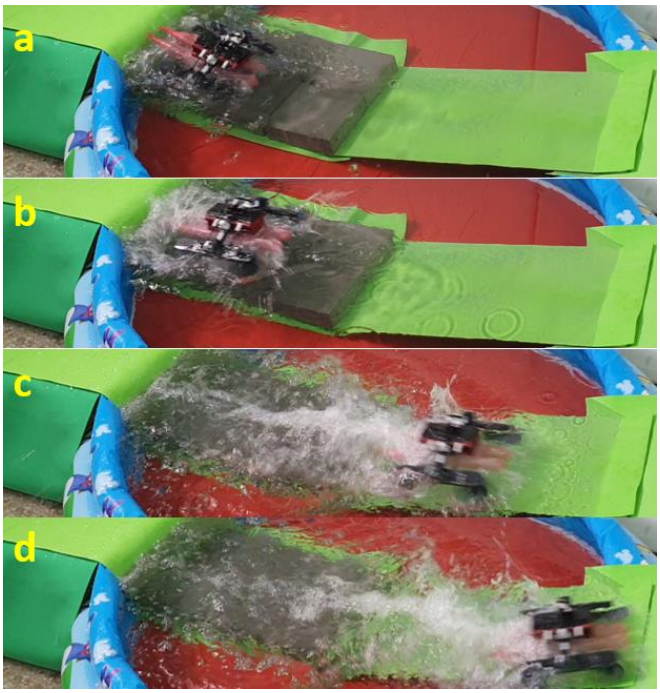

Figure 17. ASTAR running on water surface (see video).

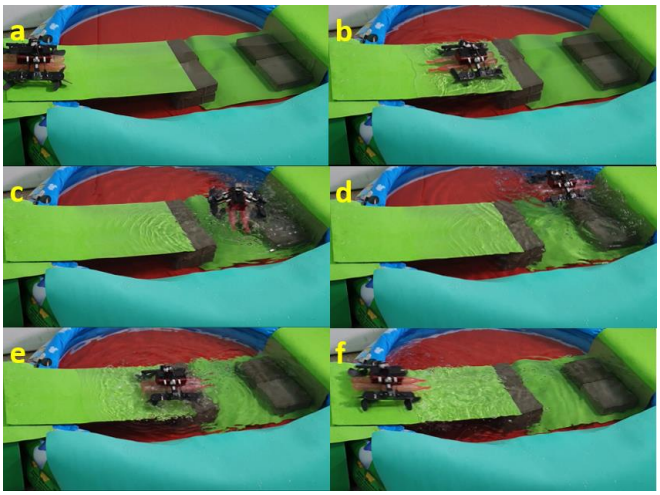

Figure 18. ASTAR transitioning from crawling to swimming and then crawling (see video).